

On a Biobased Epoxy Vitriimer from a Cardanol Derivative Prepared by a Simple Thiol-Epoxy “Click” Reaction

*Original*

On a Biobased Epoxy Vitriimer from a Cardanol Derivative Prepared by a Simple Thiol-Epoxy “Click” Reaction / Ferretti, F.; Damonte, G.; Cantamessa, F.; Arrigo, R.; Athanassiou, A.; Zych, A.; Fina, A.; Monticelli, O.. - In: ACS OMEGA. - ISSN 2470-1343. - 9:1(2024), pp. 1242-1250. [10.1021/acsomega.3c07459]

*Availability:*

This version is available at: 11583/2985100 since: 2024-01-15T22:20:00Z

*Publisher:*

American Chemical Society

*Published*

DOI:10.1021/acsomega.3c07459

*Terms of use:*

This article is made available under terms and conditions as specified in the corresponding bibliographic description in the repository

*Publisher copyright*

(Article begins on next page)

# On a Biobased Epoxy Vitrimer from a Cardanol Derivative Prepared by a Simple Thiol–Epoxy “Click” Reaction

Federico Ferretti, Giacomo Damonte, Francesco Cantamessa, Rossella Arrigo, Athanassia Athanassiou, Arkadiusz Zych, Alberto Fina, and Orietta Monticelli\*



Cite This: *ACS Omega* 2024, 9, 1242–1250



Read Online

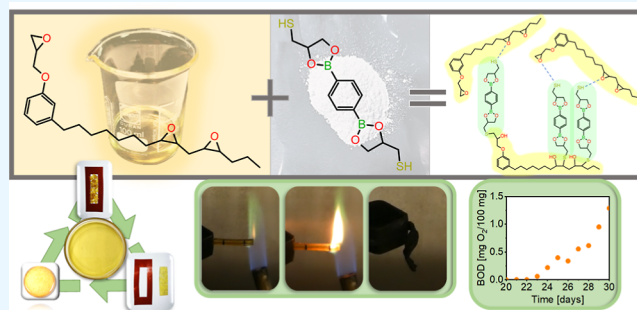
ACCESS |

Metrics & More

Article Recommendations

Supporting Information

**ABSTRACT:** The development of this work lies in the relevant interest in epoxy resins, which, despite their wide use, do not meet the requirements for sustainable materials. Therefore, the proposed approach considers the need to develop environmentally friendly systems, in terms of both the starting material and the synthetic method applied as well as in terms of end-of-life. The above issues were taken into account by (i) using a monomer from renewable sources, (ii) promoting the formation of dynamic covalent bonds, allowing for material reprocessing, and (iii) evaluating the degradability of the material. Indeed, an epoxy derived from cardanol was used, which, for the first time, was applied in the development of a vitrimer system. The exploitation of a diboronic ester dithiol ([2,2'-(1,4-phenylene)-bis[4-mercaptan-1,3,2-dioxaborolane], DBEDT) as a cross-linker allowed the cross-linking reaction to be carried out without the use of solvents and catalysts through a thiol–epoxy “click” mechanism. The dynamicity of the network was demonstrated by gel fraction experiments and rheological and DMA measurements. In particular, the formation of a vitrimer was highlighted, characterized by low relaxation times (around 4 s at 70 °C) and an activation energy of ca. 48 kJ/mol. Moreover, the developed material, which is easily biodegradable in seawater, was found to show promising flame reaction behavior. Preliminary experiments demonstrated that, unlike an epoxy resin prepared from the same monomer and using a classical cross-linker, our boron-containing material exhibited no dripping under combustion conditions, a phenomenon that will allow this novel biobased system to be widely used.



## 1. INTRODUCTION

Epoxy resins represent an important class of thermosets that are widely used in various fields such as automotive, aerospace, transportation, buildings, household, electronic and electrical equipment, etc., thanks to their excellent dimensional and thermal stability, mechanical strength, creep resistance, electrical insulation, and chemical resistance.<sup>1,2</sup> However, the permanent cross-linked structures of the material limit its ability to degrade and recycle, resulting in an increasing amount of chemical waste and significant environmental pollution.<sup>3</sup> A recent solution to this important challenge is based on the introduction of dynamic covalent bonds into the networks of epoxy resins, which has proven to be a valid method for producing reprocessable and functional epoxy thermosets.<sup>4</sup>

Indeed, in a pioneering work, this novel concept was applied to the development of epoxy-based materials by introducing transesterification catalysts into epoxy/acid or epoxy/anhydride polyester networks to form the so-called vitrimers.<sup>5</sup> In general, vitrimers are cross-linked networks containing dynamic covalent bonds, the cross-linking density of which remains unchanged when reactions take place. At low

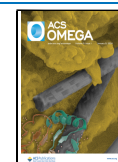
temperature, vitrimers behave as thermosets, while the reaction (e.g., transesterification) activates polymer relaxations when heated to a temperature above the topology freezing temperature ( $T_v$ ).<sup>5–7</sup> Their mechanical and self-healing properties as well as the relative  $T_g$  and  $T_v$  values can be predicted by studying vitrimers through the use of computational methods such as Monte Carlo and molecular dynamics simulations.<sup>8–11</sup> As underlined by Perego et al., the relaxation process in vitrimers is very complex and, besides temperature, was shown to depend on several parameters, such as the presence and the nature of a catalyst, bond-exchange kinetics, the monomers' structure, the dynamics of the network, and the characteristics of the molecular linkers used in linker-mediated vitrimers.<sup>10</sup> In systems where a fast exchange reaction occurs between different units, a “diffusion-limited” dynamic

**Received:** September 27, 2023

**Revised:** November 22, 2023

**Accepted:** November 23, 2023

**Published:** December 21, 2023



relaxation type takes place; i.e., the rate-determining step of the relaxation process is related to the mobility of the network, which in turn affects the ability of the groups giving exchange reactions to meet. Conversely, in the cases where particularly slow bond-exchange reactions occur, a relaxation phenomenon of the “chemically limited” type occurs, i.e., where the relaxation process is precisely limited by the kinetics of exchange between the reactive groups. In particular, epoxy-based vitrimers, classified according to the exchangeable bonds and reactions in their cross-linked networks, are generally based on disulfide bonds<sup>12,13</sup> and the corresponding disulfide-exchange reaction,<sup>13</sup> imine bonds<sup>14</sup> and the corresponding transamination and imine metathesis, siloxane equilibration,<sup>15,16</sup> and on ester bonds and the corresponding transesterification,<sup>5,17–21</sup> with the latter approach being the most commonly used. Indeed, in order to accelerate the exchange reaction in epoxy/acid and epoxy/anhydride systems, zinc acetate,<sup>17,18</sup> zinc acetylacetonate,<sup>19</sup> triazabicyclodecene,<sup>20,21</sup> and other transesterification catalysts were used, which, although added in limited amounts, can introduce a potential toxicity risk and reduce the thermomechanical stability of the material. On this basis, the use of the catalyst is a relevant drawback that was attempted to be solved by introducing hydroxyl groups and tertiary amine groups to activate the exchange of dynamic bonds in the preparation of epoxy vitrimers with a catalyst-free transesterification mechanism.<sup>22,23</sup>

Therefore, the use of boronic esters as cross-linkers is of great interest since they can be used in the preparation of dynamic networks without the use of catalysts owing to their ability to introduce bond exchange through transesterification and metathesis reactions characterized by very low activation energies.<sup>24,25</sup> In particular, among this class of compounds, the exchange property of the five-membered cyclic dioxaborolane unit, which can be easily obtained from the condensation of differently substituted boronic acids and diols, is particularly useful and they were used in several systems due to their good chemical and thermal stability. Indeed, in a pioneering work, Röttger et al. proposed an innovative approach to prepare vitrimers from thermoplastics by copolymerization or grafting of ad hoc prepared dynamic dioxaborolane-containing cross-linkers to the polymer chains.<sup>26</sup> By exploiting the same concept, Ricarte et al. developed polyethylene-based vitrimers in a melt extrusion process by grafting a dioxaborolane bismaleimide derivative dynamic cross-linker in different molar ratios onto polyethylene chains. Significant differences in both crystallinity and rheological properties were highlighted for these systems compared to the starting polymer.<sup>27,28</sup>

Another important challenge in the development of these materials, related to the increasing concern about the reduction need of nonrenewable fossil fuels and environmental issues, is the production of biobased epoxy resins.<sup>29</sup> Indeed, recently, the preparation of epoxy vitrimers from renewable sources was considered as this approach counteracts both fossil resource and CO<sub>2</sub> emission depletion. In particular, Yang et al. described a biobased vitrimer curing epoxy soybean oil and fumaropimaric acid preparation, which showed a  $T_g$  and tensile strength of 65 °C and 16.0 MPa, respectively.<sup>30</sup> Epoxidized soybean oil in the acrylated form was also applied by Zych et al., who produced a vitrimer system by thiol–acrylate coupling between the oil and a diboronic ester dithiol.<sup>31</sup> Tung oil-based triglycidyl ester and citric acid were used by Xu et al. to develop a biobased epoxy vitrimer, characterized by good self-healing, recyclability, and shape memory properties.<sup>32</sup> More

recently, biobased and recyclable epoxy vitrimers were prepared from ferulic acid-derived epoxy resin, ferulic acid-based hyperbranched epoxy resin, and citric acid without using a catalyst. For the final formulation, an activation energy and a relaxation time at 140 °C of 58 kJ/mol and 45 s, respectively,<sup>33</sup> was reported. Concerning composite vitrimers, Liu et al. reported the preparation of carbon fiber-reinforced biobased epoxy vitrimers and described that the regenerated-carbon fiber-reinforced composites exhibited insignificant differences with respect to the composites reinforced with virgin fibers, even after multiple recoveries.<sup>34</sup> In the same field, carbon nanotubes were combined with biobased epoxy vitrimers cured with cashew nutshell liquid and citric acid,<sup>35</sup> and the developed nanocomposite vitrimers demonstrated good anticorrosion performance on a steel substrate.<sup>35</sup>

In this work, considering the potential of biomaterials for the development of novel vitrimer systems, a cardanol-based epoxide was investigated. With the aim of preparing these materials without the use of solvents, a cross-linker, namely, [2,2'-(1,4-phenylene)-bis[4-mercaptan-1,3,2-dioxaborolane] (DBEDT), was used, which is potentially capable of forming bonds between thiol and epoxide by a kind of “click” reaction that can be efficiently carried out under relatively mild and solventless conditions, proceeding with high conversion and without the use of catalysts (Figure 1).<sup>36–38</sup> The novelty of this

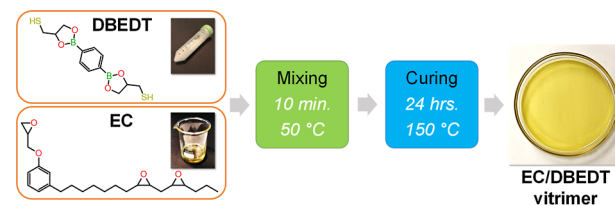


**Figure 1.** Scheme of the cardanol-based epoxy (EC) cross-linking reaction.

work is not only the particular type of compound used but also, among other properties, the behavior of flame retardancy, which is not usually studied for this recent class of materials.

## 2. EXPERIMENTAL SECTION

**2.1. Materials.** Cardanol-based epoxy (GX-2551, Figure 1), termed EC, was provided by Cardolite Corporation (USA). EC was characterized by a viscosity at 25 °C of 102 cP, while the epoxy equivalent weight was 170 g/g equiv epoxy. Pripol 1006, dimer acid hydrogenated was provided by Croda Coatings & Polymers (acid value 196 mg KOH/g). Benzene-1,4-diboronic acid, 1-thioglycerol (97%), ethanol (EtOH, 96%), and anhydrous toluene (99.8%) were purchased from Merck and used as received unless otherwise stated. The cross-linker, namely, [2,2'-(1,4-phenylene)-bis[4-mercaptan-1,3,2-dioxaborolane] (DBEDT), was prepared by following the procedure previously reported.<sup>31</sup>

**2.2. Epoxy Cross-Linking Procedure.** Both reagents, DBEDT and EC, were kept in a desiccator for 48 h prior to be used. DBEDT, which is a fairly coarse powder, was finely ground to improve mixing with EC. The stoichiometric ratio between the reactants was chosen to be 1:1 based on the reactive groups. Epoxy cross-linking was performed in two steps. In the first step, EC was added to a 250 mL flask, equipped with a mechanical stirrer, that had previously been heated to 50 °C in a silicone oil bath. This procedure was used to reduce the

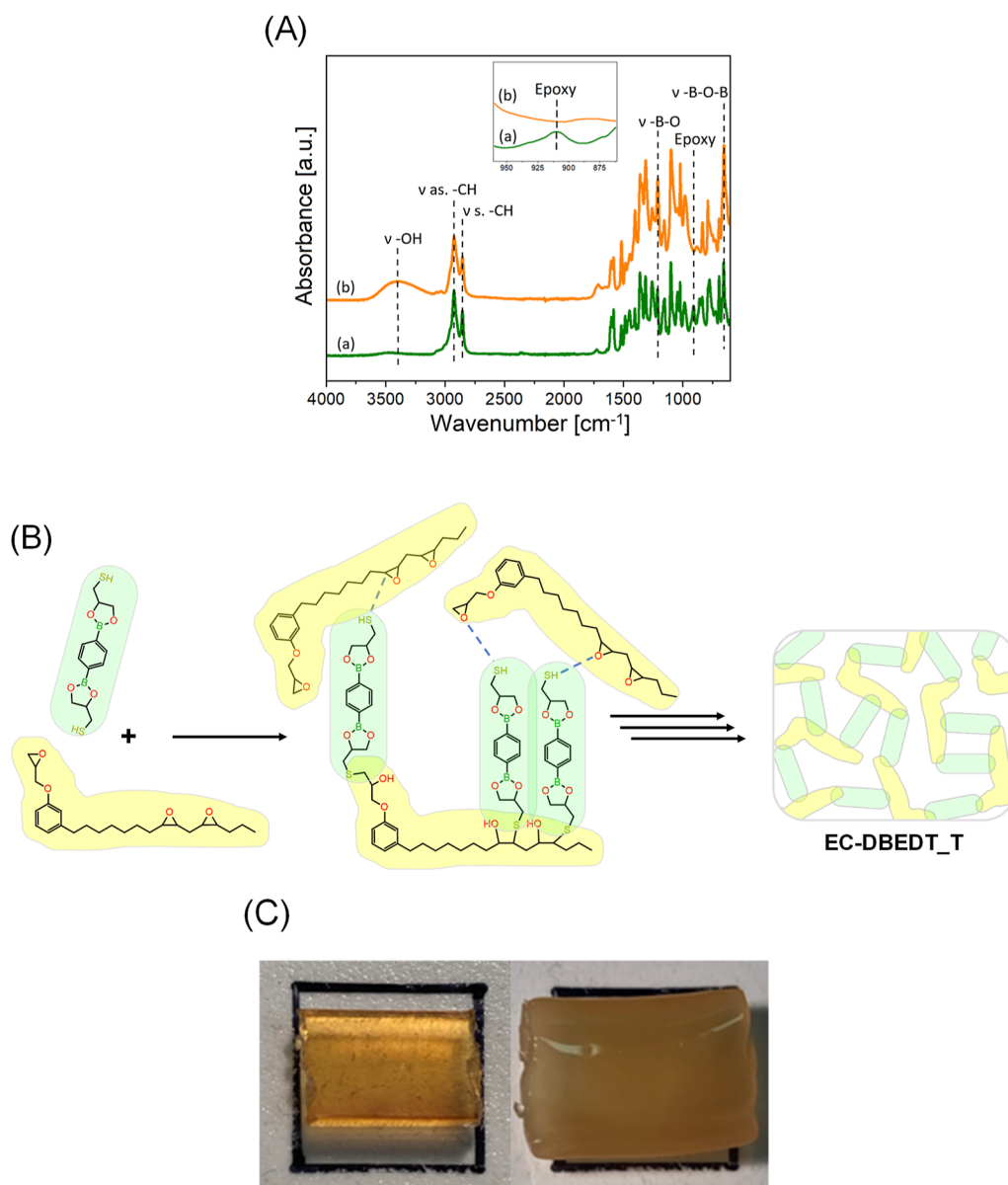


**Figure 2.** (A) FT-IR spectra of (a) neat mixture EC-DBEDT and (b) thermally treated EC-DBEDT mixture (EC-DBEDT\_T). (B) Scheme of the “click reaction” between EC and DBEDT. (C) Photos of left neat EC-DBEDT\_T and right swollen EC-DBEDT\_T in anhydrous toluene.

viscosity of the reagent and ensure better mixing. DBEDT was then added to the flask, and the system was stirred for 10 min, during which time it changed from an initially pasty system to a whitish liquid. The actual curing reaction took place in the second phase, in which the mixture was poured into special silicone molds and placed in an oven at 150 °C for 24 h. The same procedure was used to prepare a sample cross-linked with Pripol 1006.

**2.3. Characterization Measurements.** Fourier transform infrared (FT-IR) spectra of the prepared samples were recorded in ATR from 400 to 4000 cm<sup>-1</sup> using a Bruker “Vertex 70”.

Differential scanning calorimetry (DSC) measurements were performed with a Mettler Toledo calorimeter (DSC1 STARE System) calibrated with high-purity indium and operated under a flow of nitrogen. The weight of the samples was about 5 mg, and a scanning rate of 10 °C/min was employed in all the runs. The samples were heated from 25 to 200 °C, then cooled down to -100 °C, and finally heated up again to 200

°C. The reported glass transition temperature ( $T_g$ ) value was defined as the midpoints of the sigmoidal curve and maxima of the endotherms, respectively.

Thermal gravimetric analysis (TGA) was performed using a STARE System Mettler thermobalance under a flow of nitrogen or air of 80 mL/min. The weight loss of the samples (having initial masses of ca. 10 mg) was measured from room temperature to 800 °C at a heating rate of 10 °C/min.

The gel fraction (GF %) and swelling ratio (SR %) were evaluated using anhydrous toluene, a solvent capable of dissolving both the mixture reagents. For this purpose, about 70 mg of the samples were accurately weighed and contacted with 3 mL of anhydrous toluene for 24 h. The samples were then collected and first dried for 6 h at 25 °C and atmospheric pressure and then stored in an oven at 30 °C for 24 h under vacuum to completely remove the solvent.

The samples were weighed, and the GF % was calculated using eq 1.

$$\text{GF \%} = M_d / M_i \times 100 \quad (1)$$

where  $M_d$  is the weight of the dried sample and  $M_i$  is its initial weight.

To calculate SR %, the samples were weighed after 24 h of contact with toluene anhydrous, and eq 2 was applied.

$$\text{SR \%} = (M_{\text{wet}} - M_d) / M_d \times 100 \quad (2)$$

where  $M_{\text{wet}}$  is the weight of the swollen polymer and  $M_d$  is the weight of the dried sample.

Recycling tests were performed on specimens 1 cm in diameter and 1 mm in thickness. The specimens were divided into fragments and placed in a brass mold of  $3.0 \times 3.5 \text{ cm}^2$  and a depth of  $250 \mu\text{m}$  and then pressed for 15 min at 3 MPa and  $120 \text{ }^\circ\text{C}$ .

Dynamic mechanical thermal analysis (DMTA) was carried out on bars (cross-section  $6 \times 1 \text{ mm}^2$ , 30 mm length) obtained from compression-molded plates in tensile mode on a TA Instruments Q800.  $2 \text{ }^\circ\text{C}/\text{min}$  heating rate was applied from room temperature up to  $180 \text{ }^\circ\text{C}$  at 1 Hz frequency in strain-controlled mode, deformation amplitude at 0.05% and 0.01 N preload. Samples were conditioned at  $23 \text{ }^\circ\text{C}$  and 50% of relative humidity for at least 48 h before analyses.

Rheological analysis was carried out on a TA Instruments ARES rheometer operated with a 25 mm parallel plate geometry and 1 mm thickness samples. Dynamic frequency sweep tests were carried out to determine  $G'$ ,  $G''$ , and complex viscosity ( $\eta^*$ ) between 0.1 and 100 rad/s at 1% strain (linear viscoelasticity) under isothermal condition, in the range between 120 and  $210 \text{ }^\circ\text{C}$ . Isothermal relaxation tests were also carried out at 1% strain. Stress  $G(t)$  is reported normalized on  $G_0$ , i.e., the stress recorded at  $t = 0.1 \text{ s}$  to get rid of instrumental transient at the start for the relaxation test. Rheological tests were performed with a nitrogen flux to avoid hydrolytic degradation.

Flammability test was performed in a horizontal configuration by the application of a 20 mm blue methane flame for 10 s on  $3 \times 1 \times 30 \text{ mm}^3$  specimens. During combustion, the formation of molten incandescent polymer drops was evaluated.

The biodegradability of the samples was evaluated by biochemical oxygen demand (BOD), which can be easily determined by monitoring the oxygen consumption in a closed respirometer. Specifically, approximately 200 mg of the sample was added to 432 mL of seawater as the sole carbon source. The seawater was chosen to mimic real environmental conditions. Indeed, it already contains microbial consortia and saline nutrients required for their growth. The experiment was conducted at RT in dark glass bottles with a volume of 510 mL, hermetically closed with an OxiTop measuring head. A  $\text{CO}_2$  scavenger was added to trap carbon dioxide produced during biodegradation, and biotic consumption of oxygen present in the free volume of the system was measured as a function of pressure drop. Samples were tested in duplicate. Raw data of oxygen consumption ( $\text{mg O}_2/\text{L}$ ) were corrected by subtracting the mean of blank values, obtained by measuring seawater oxygen consumption in the absence of test material. After this subtraction, the values were normalized to the mass of each sample and referred to 100 mg of material ( $\text{mg O}_2/100 \text{ mg}$ ).

### 3. RESULTS AND DISCUSSION

The comparison of the FT-IR spectra of the mixture of the neat cardanol-based epoxy resin (EC) and DBEDT and the same mixture subjected to a heat treatment at  $150 \text{ }^\circ\text{C}$  for 24 h (EC-DBEDT\_T), shown in Figure 2A, served to confirm the occurrence of the cross-linking reaction. The above curing temperature was chosen to promote the cross-linking but limit the thermal decomposition of the material. In both spectra, the presence of the boronic acid ester is evidenced by the stretching of the B-O and the B-O-B bonds at  $1211$  and  $655 \text{ cm}^{-1}$ , respectively, belonging to DBEDT.<sup>39</sup> In addition, the signals at  $2925$  and  $2853 \text{ cm}^{-1}$  can be attributed to the asymmetric and symmetric stretching of the  $\text{C}(\text{sp}^3)\text{-H}$  bonds, respectively. Apart from the bands mentioned above, which are present in both the neat and the treated mixture, some differences are visible. A first observation refers to the broadened band in the thermally treated mixture, in the range between about  $3100$  and  $3700 \text{ cm}^{-1}$ . This signal, associated with the stretching of hydroxyl groups, can be attributed to the formation of hydroxyl functionalities originating from the reaction between thiol groups and epoxides (Figures 2B and S1).<sup>36-38,40</sup>

Moreover, it was found that the signal visible in the neat mixture at  $910 \text{ cm}^{-1}$ , which can be attributed to the epoxide groups,<sup>41</sup> disappears in the treated EC-DBEDT (see the inset of Figure 2A). The above finding is also indicative of the occurrence of the reaction between EC and DBEDT under the applied conditions, which is shown in Figure 2B.

To support the formation of a three-dimensional network, a GF test was performed in anhydrous toluene after checking the solubility of the starting reagents in this solvent. Figure 2C shows the photographs of the starting sample and the material after 24 h in contact with the solvent. It is worth mentioning that this test allowed the evaluation of gel content (GF %) and SR %, which were 99% and 188%, respectively. These findings, together with the results of FT-IR characterization, prove a complete yield and effective cross-linking of the material owing to the reaction between EC and DBEDT (Figure 2B). It is worth underlining that variable GF % was previously reported for epoxy-based vitrimers. For example, vitrimers prepared from sebacic acid and diglycidyl ether of bisphenol A, with zinc acetylacetonate as the catalyst for the exchange reaction, reached a GF % of about 80% at a temperature and time comparable with those used for the preparation of our material, i.e.,  $160 \text{ }^\circ\text{C}$  and 24 h.<sup>42</sup> In the case of epoxidized soybean oil-derived vitrimers, prepared using 4,4'-dithiodiphenylamine as a curing agent and a curing time of 20 h and  $160 \text{ }^\circ\text{C}$  of curing temperature, a GF % of only 54% was obtained.<sup>43</sup> In this case, the GF could be increased only by increasing the temperature and curing time. Nevertheless, at  $180 \text{ }^\circ\text{C}$  and with a curing time of about 28 h, a maximum value of about 80% was achieved. Comparing these results with the GF % value obtained in our work, it can be concluded that the cross-linking system used is extremely effective and allows complete cross-linking without the need to further increase the temperature. This limits problems related to the stability of the material and to secondary reactions and makes the preparation procedure more easily scalable. Moreover, it can be deduced from the photo of the swollen sample that the high degree of swelling is associated with the retention of the shape of the sample, which is a typical feature of vitrimer systems.<sup>4</sup>

The glass transition temperature of the cured mixture was studied by comparing the DSC traces of neat EC and EC–DBEDT\_T (Figure 3a and Table 1). In contrast to the starting

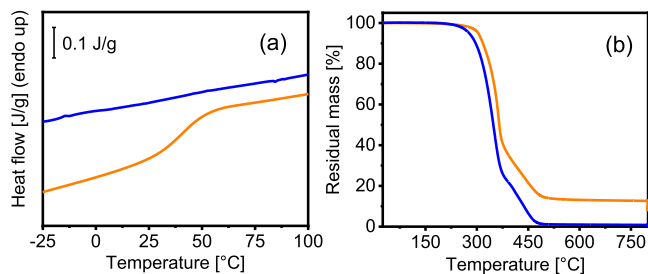


**Figure 3.** (a) DSC traces of blue EC and orange EC–DBEDT\_T. (b) TGA curve of blue EC and orange EC–DBEDT\_T.

**Table 1. Thermal Properties of the EC and EC\_DBEDT\_T<sup>a</sup>**

sample code	$T_{g_i}$ [°C]	$T_{onset}$ [°C]	$T_{max1}$ [°C]	$T_{max2}$ [°C]	residual weight [%]
EC		277	350	439	0
EC–DBEDT_T	45	304	364	438	15

<sup>a</sup> $T_{onset}$  and  $T_{max}$  indicate the onset of the degradation temperature at a weight loss of 5% and the maximum rate of degradation temperature, respectively.

cardanol-based epoxy sample, which showed no signal in the range from  $-25$  to  $100$  °C, the cured mixture exhibited a glass transition temperature ( $T_g$ ) of  $45$  °C, reflecting the relatively high mobility of alkylic chains in cardanol. This finding confirms the formation of macromolecular chains during the cross-linking reaction.

The thermal stability of EC–DBEDT\_T and neat EC was studied by TGA analysis at a heating rate of  $10$  °C/min under a nitrogen atmosphere. The TGA curves of the analyzed samples are shown in Figure 3b, while the results are summarized in Table 1, where the onset decomposition temperature ( $T_{onset}$ ) and the temperature of the maximum rate of decomposition ( $T_{max}$ ) as well as the residual weight are also given. Both EC and EC–DBEDT\_T showed two degradation steps characterized by different  $T_{max}$ . As previously reported in the literature, the first weight loss step can be attributed to the breakdown and volatilization of the EC chains, while a higher stability fraction is decomposed at a higher temperature in the second weight loss step.<sup>44,45</sup> It was found that the material cross-linking slightly affects the  $T_{onset}$  and  $T_{max1}$ , corresponding to the first degradation step,  $T_{onset}$  going from  $277$  to  $304$  °C and  $T_{max1}$  from  $350$  to  $364$  °C for EC and EC–DBEDT\_T, respectively. While the starting epoxy did not show any residue at high temperatures, it is relevant to underline that the degradation of the cross-linked material leads to the formation of a significant residual weight (about 15%). This suggests a partial charring of the cross-linked polymer, in competition with its volatilization, possibly related to the action of the boronic compound, as boron is a well-known charring promoter, which is expected to positively affect the performance in the reaction to a flame exposure.<sup>46,47</sup> TGA analysis was also performed under an oxidizing atmosphere, in air, and the results are shown in the Supporting Information (Figure S2). The TGA profile of EC shows three weight loss steps. Indeed, in addition to the two steps previously observed in an inert atmosphere, it appears that the presence of oxygen promotes the formation of a limited amount of a carbonaceous phase

upon the main decomposition steps, yielding approximately 10% residue at  $400$  °C, which is subsequently oxidized leading to a negligible residue above  $600$  °C. On the other hand, EC–DBEDT\_T decomposes, yielding 40% of charred residue at  $400$  °C, which is then progressively decomposed by oxidation at higher temperature, still retaining approximately 15% of the initial weight at  $750$  °C. The porous char residue recovered after TGA in air was analyzed by means of FT-IR (Figure S3). The presence of several bands at  $3190$ ,  $1406$ ,  $1192$ ,  $705$ , and  $638$   $\text{cm}^{-1}$  in the spectrum, which can be attributed to the stretching of B–OH bonds and tri- and tetracoordinated B–O units, is consistent with the presence of boron oxide,<sup>48–50</sup> thus supporting the role of boron compounds in the organization of a stable charred residue.

Viscoelastic properties for EC–DBEDT\_T were studied as a function of the temperature by dynamic mechanical analysis and oscillatory rheology to investigate the relaxation dynamics. DMTA (Figure 4) exhibits the peak of main chain relaxation

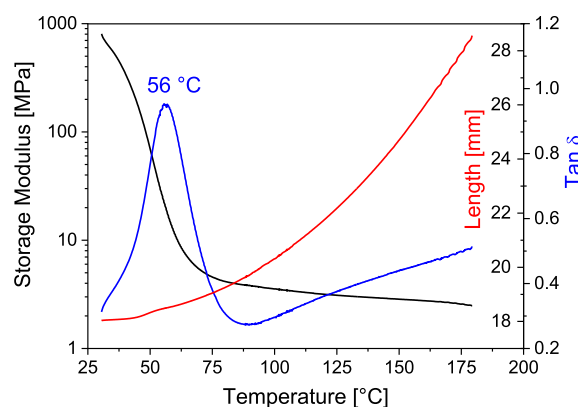


**Figure 4.** DMTA results (storage modulus,  $\tan \delta$ , and length as a function of temperature) for EC–DBEDT\_T.

( $T_a$ ) at approximately  $56$  °C, taken as the maximum of  $\tan \delta$ , in fair agreement with the glass transition temperature measured in DSC. Above the main relaxation, a rubbery state is observed, with storage modulus in the range of a few megapascals. Indeed, the rubbery state does not produce a stable plateau but rather a slowly decreasing curve, ranging between approximately  $4$  MPa at  $80$  °C and  $2.5$  MPa at  $180$  °C. This decreasing trend appears to be related to the elongation of the sample, which is higher than that for expected linear thermal expansion. This suggests that the sample is actually starting to flow under its own weight under the testing condition, which represents a first evidence of its fast relaxation above  $T_a$ .<sup>31</sup>

To further investigate the viscoelastic properties at higher temperatures, plate–plate oscillatory rheology was carried out. In Figure 5a, storage modulus ( $G'$ ) and loss modulus ( $G''$ ) are reported as a function of frequency at different temperatures. The shape of  $G'$  reflects the relaxation of the system at low frequencies, which becomes faster at higher temperatures, as shown by the increasing slope of the  $G'$  plot in the low-end frequency range. Furthermore, the crossover between  $G'$  and  $G''$  shifts toward higher-frequency values with increasing temperature, namely, at  $0.6$ ,  $1.2$ ,  $2.6$ , and  $6.6$  rad/s for  $120$ ,  $150$ ,  $180$ , and  $210$  °C, respectively. This confirms that the material shifts toward a dominant viscous behavior with increasing temperature.

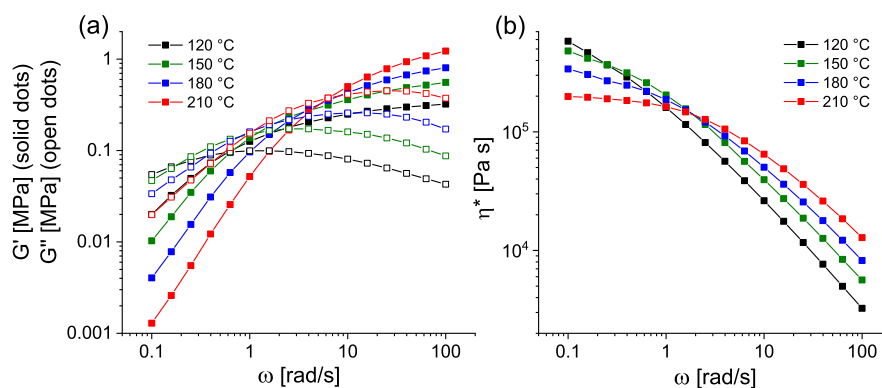


**Figure 5.** (a) Elastic ( $G'$ ) and viscous ( $G''$ ) moduli and (b) complex viscosity as a function of frequency measured by dynamic frequency sweep tests performed at different temperatures.

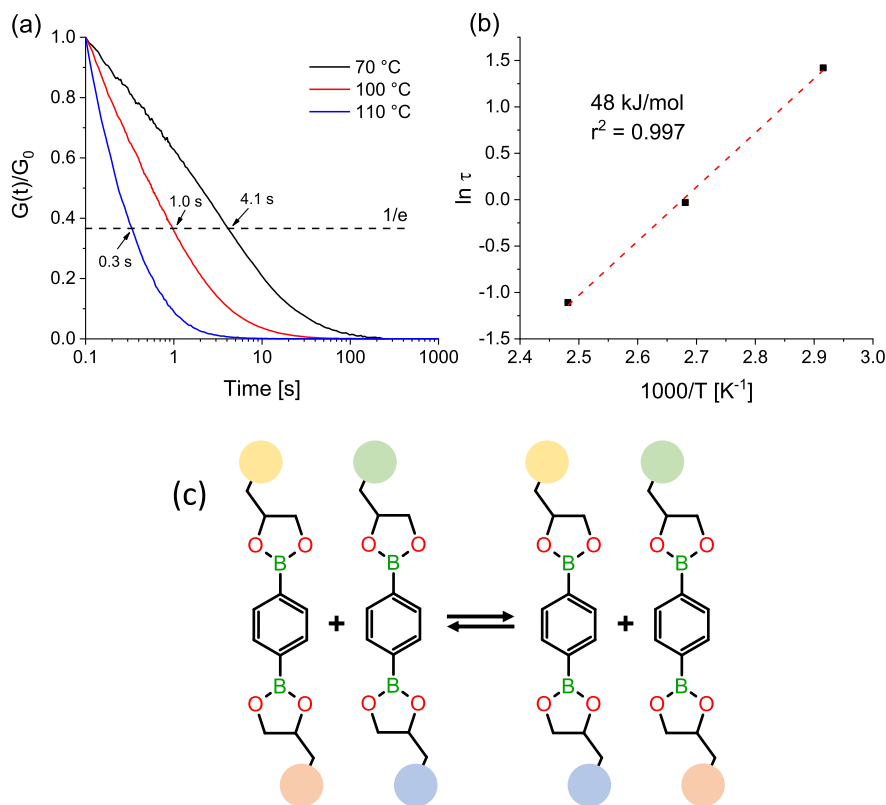


**Figure 6.** (a) Stress relaxation curves; (b) variation of the stress relaxation time vs inverse temperature; and (c) boronic ester metathesis exchange reaction.

These observations were further confirmed by the viscosity plots (Figure 5b), which show a progressively more defined Newtonian plateau with increasing temperature. As the relaxation of a covalent associative network depends on the dynamics of bond exchanges, stress relaxation tests were also carried out, and relaxation times (Figure 6a) were used to calculate the apparent activation energy for the relaxation, according to Arrhenius plots (Figure 6b). The results reported in Figure 6a showed very short relaxation times in the range of a few seconds in the temperature range between 70 and 130 °C, suggesting bond exchange to be effective for the network relaxation as soon as cooperative movement of the macromolecules is possible, i.e., just above the  $T_g$ . The calculated activation energy is approximately 48 kJ/mol, which is in the same range as the previously reported systems based on the boronic ester metathesis exchange reaction (Figure 6c).<sup>26,31</sup>

The observed extremely rapid stress relaxation behavior can be explained by considering the high segmental mobility of the macromolecular chains above  $T_g$  and the very fast kinetics of the exchange reactions.

Since recyclability is one of the main advantages of vitrimers over conventional epoxy resins, this property was tested for the system developed in this work. Indeed, the above feature meets the recent demand for circular economy since recycled materials can be reintroduced in the market and reduce both waste and the need for raw materials. To demonstrate recyclability, the developed films were first fractured into small pieces, which were subsequently collected in a rectangular-shaped mold, where hot pressing was applied. The test was performed under a pressure of 3 MPa, which is rather low compared to the pressure normally used for tests with similar systems.<sup>40</sup> After hot pressing at 150 °C for 15 min,

i.e., the same temperature as that for curing, the fractured pieces were reassembled again into a film (Figure 7a).

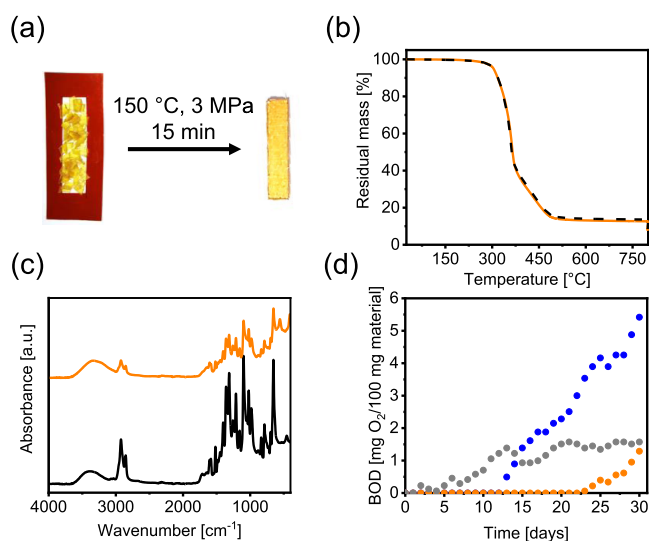


**Figure 7.** (a) Photo of the broken sample and recycled film. (b) TGA curves of the black neat EC-DBEDT<sub>T</sub> sample and orange EC-DBEDT<sub>T</sub> after the recycle step. (c) FT-IR curves of the black neat EC-DBEDT<sub>T</sub> sample and orange EC-DBEDT<sub>T</sub> after the recycle step. (d) BOD of EC (blue), EC-DBEDT<sub>T</sub> (orange), and microcrystalline cellulose (biodegradable reference) (gray).

This phenomenon indicates that sufficient bond exchange and chain interpenetration had occurred among the broken pieces. In addition, the TGA curves (Figure 7b) and the FT-IR spectra (Figure 7c) for the recycled films coincide well with those of the neat films, indicating that the chemical structures were maintained after the recycling processes.

The biodegradability of cardanol-based vitrimer was tested in the marine environment by BOD analysis (Figure 7d), comparing the behavior of EC-DBEDT<sub>T</sub> with that of EC and microcrystalline cellulose, a well-known biodegradable material. The biodegradation of EC-DBEDT<sub>T</sub> was first detected after 22 days of immersion with seawater, and within 1 month, BOD reached a value of 1.3 mg O<sub>2</sub>/100 mg. Conversely, the biodegradation of the starting cardanol-based epoxy, EC, was detected much earlier (12 days) and showed a higher value of 5.4 mg O<sub>2</sub>/100 mg at the end of the test (30

days). The initial delay in the biodegradation of the vitrimer described above can be ascribed to its cross-linked structure and the fact that boronic ester bonds must be hydrolyzed before biodegradation can occur. Nevertheless, it is relevant to underline that after 30 days, the vitrimer sample reached a BOD value of 1.6 mg O<sub>2</sub>/100 mg, which is similar to that of the reference material, namely, the microcrystalline cellulose. The comparison of the behavior of our material with that of other systems based on cardanol derivatives is not straightforward since degradation depends specifically on the type of compound used as well as on the degradation procedure applied. For example, the biodegradability of cardanol-based compounds used as plasticizers of poly(vinyl chloride) was found to be higher than that of cardanol when activated sludge was used as microbial biomass for the test,<sup>51</sup> proving the tendency of the above-mentioned materials to be easily biodegraded. Moreover, the results obtained with our materials are very interesting as they show that the incorporation of a cardanol-based compound into a dynamic network based on hydrolyzable boronic esters does not limit its ability to decompose under environmental conditions.

Another interesting property of the developed materials that was evaluated was their flammability behavior. In particular, the behavior of the vitrimer was compared with a permanently cross-linked system prepared with a conventional cross-linker, i.e., Pripol 1006. Figure 8 shows snapshots of the test specimens during combustion. These preliminary results indicated a significant difference between the two materials. While the vitrimer film burned without dripping, leaving a significant charred residue on the tongs, the combustion of Pripol-based epoxy led to significant dripping with no residue. As dripping is correlated with flame propagation in a real fire scenario, stopping the detachment of inflamed parts of the specimen is indeed interesting and may be attributed to the charring induced by the boron-based compounds, as suggested by TGA and FT-IR analysis, which are known to be potentially active flame retardants for polymers and for epoxy resins in particular.<sup>52–55</sup>

#### 4. CONCLUSIONS

In this work, a vitrimer system was developed by using a reagent from renewable sources as well as an environmentally friendly manufacturing process that does not require catalysts or solvents, is easily scalable, and could be applied to other

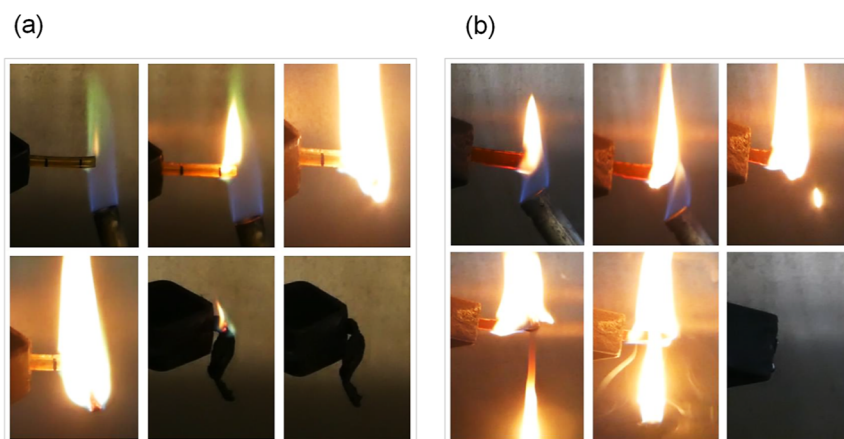


**Figure 8.** Photos of the combustion of (a) vitrimer EC-DBEDT<sub>T</sub> and (b) Pripol-based resin.



types of epoxy-based compounds. The network prepared, starting from a cardanol-derivative epoxy, is characterized by very short relaxation times due to the rapid boronic ester metathesis exchange reaction. The above feature allowed the vitrimer to be easily thermomechanically recyclable, with its thermal and chemical properties remaining unchanged after the recycling process. Moreover, the developed vitrimer shows an interesting combustion behavior, burning without dripping, a phenomenon that can be attributed to the presence of boron-based compounds in the network.

The biobased nature of the starting epoxy, the environmentally friendly and easily scalable production method, the recyclability and seawater biodegradability, as well as the flammability behavior make the materials developed in this paper extremely promising for practical applications where fully circular end-of-life products are required.

## ■ ASSOCIATED CONTENT

### SI Supporting Information

The Supporting Information is available free of charge at <https://pubs.acs.org/doi/10.1021/acsomega.3c07459>.

Thiol–epoxy reaction scheme; TGA thermograms in air of EC–DBEDT\_T and EC; and FT-IR spectrum of the leftover residue after TGA in air of EC–DBEDT\_T (PDF)

## ■ AUTHOR INFORMATION

### Corresponding Author

Orietta Monticelli – Dipartimento di Chimica e Chimica Industriale, Università degli studi di Genova, 16146 Genoa, Italy; [orcid.org/0000-0003-4999-3069](https://orcid.org/0000-0003-4999-3069); Email: [orietta.monticelli@unige.it](mailto:orietta.monticelli@unige.it)

### Authors

Federico Ferretti – Dipartimento di Chimica e Chimica Industriale, Università degli studi di Genova, 16146 Genoa, Italy

Giacomo Damonte – Dipartimento di Chimica e Chimica Industriale, Università degli studi di Genova, 16146 Genoa, Italy

Francesco Cantamessa – Dipartimento di Scienza Applicata e Tecnologia, Politecnico di Torino, 15121 Alessandria, Italy

Rossella Arrigo – Dipartimento di Scienza Applicata e Tecnologia, Politecnico di Torino, 15121 Alessandria, Italy; [orcid.org/0000-0002-0291-2519](https://orcid.org/0000-0002-0291-2519)

Athanassia Athanassiou – Smart Materials, Istituto Italiano di Tecnologia, 16163 Genoa, Italy; [orcid.org/0000-0002-6533-3231](https://orcid.org/0000-0002-6533-3231)

Arkadiusz Zych – Smart Materials, Istituto Italiano di Tecnologia, 16163 Genoa, Italy; [orcid.org/0000-0001-7814-2584](https://orcid.org/0000-0001-7814-2584)

Alberto Fina – Dipartimento di Scienza Applicata e Tecnologia, Politecnico di Torino, 15121 Alessandria, Italy; [orcid.org/0000-0002-8540-6098](https://orcid.org/0000-0002-8540-6098)

Complete contact information is available at:

<https://pubs.acs.org/doi/10.1021/acsomega.3c07459>

### Author Contributions

The manuscript was written through contributions of all authors. All authors have given approval to the final version of the manuscript.

## Notes

The authors declare no competing financial interest.

## ■ ACKNOWLEDGMENTS

The authors acknowledge the company AEP Polymers S.r.l. for having provided some of the reagents used in this work.

## ■ REFERENCES

- (1) Jin, F.-L.; Li, X.; Park, S.-J. Synthesis and application of epoxy resins: a review. *J. Ind. Eng. Chem.* **2015**, *29*, 1–11.
- (2) Auvergne, R.; Caillol, S.; David, G.; Boutevin, B.; Pascault, J.-P. Biobased thermosetting epoxy: present and future. *Chem. Rev.* **2014**, *114*, 1082–1115.
- (3) Shieh, P.; Zhang, W.; Husted, K. E. L.; Kristufek, S. L.; Xiong, B.; Lundberg, D. J.; Lem, J.; Veysset, D.; Sun, Y.; Nelson, K. A.; Plata, D. L.; Johnson, J. A. Cleavable comonomers enable degradable, recyclable thermoset plastics. *Nature* **2020**, *583*, 542–547.
- (4) Yang, Y.; Xu, Y.; Ji, Y.; Wei, Y. Functional epoxy vitrimers and composites. *Prog. Mater. Sci.* **2021**, *120*, 100710.
- (5) Montarnal, D.; Capelot, M.; Tournilhac, F.; Leibler, L. Silica-like malleable materials from permanent organic networks. *Science* **2011**, *334*, 965–968.
- (6) Capelot, M.; Unterlass, M. M.; Tournilhac, F.; Leibler, L. Catalytic control of the vitrimer glass transition. *ACS Macro Lett.* **2012**, *1*, 789–792.
- (7) Capelot, M.; Montarnal, D.; Tournilhac, F.; Leibler, L. Metal-catalyzed transesterification for healing and assembling of thermosets. *J. Am. Chem. Soc.* **2012**, *134*, 7664–7667.
- (8) Singh, G.; Sundararaghavan, V. Modeling self-healing behavior of vitrimers using molecular dynamics with dynamic cross-linking capability. *Chem. Phys. Lett.* **2020**, *760*, 137966.
- (9) Perego, A.; Khabaz, F. Volumetric and rheological properties of vitrimers: a hybrid molecular dynamics and monte carlo simulation study. *Macromolecules* **2020**, *53*, 8406–8416.
- (10) Perego, A.; Lazarenko, D.; Cloitre, M.; Khabaz, F. Microscopic dynamics and viscoelasticity of vitrimers. *Macromolecules* **2022**, *55*, 7605–7613.
- (11) Zhao, H.; Wei, X.; Fang, Y.; Gao, K.; Yue, T.; Zhang, L.; Ganesan, V.; Meng, F.; Liu, J. Molecular dynamics simulation of the structural, mechanical, and reprocessing properties of vitrimers based on a dynamic covalent polymer network. *Macromolecules* **2022**, *55*, 1091–1103.
- (12) Ruiz de Luzuriaga, A.; Matxain, J. M.; Ruipérez, F.; Martin, R.; Asua, J. M.; Cabañero, G.; Odriozola, I. Transient mechanochromism in epoxy vitrimer composites containing aromatic disulfide crosslinks. *J. Mater. Chem. C* **2016**, *4*, 6220–6223.
- (13) Guggari, S.; Magliozzi, F.; Malburet, S.; Graillet, A.; Destarac, M.; Guerre, M. Vanillin-based epoxy vitrimers: looking at the cystamine hardener from a different perspective. *ACS Sustain. Chem. Eng.* **2023**, *11*, 6021–6031.
- (14) Wang, S.; Ma, S.; Li, Q.; Xu, X.; Wang, B.; Yuan, W.; Zhou, S.; You, S.; Zhu, J. Facile in situ preparation of high-performance epoxy vitrimer from renewable resources and its application in non-destructive recyclable carbon fiber composite. *Green Chem.* **2019**, *21*, 1484–1497.
- (15) Wu, X.; Yang, X.; Yu, R.; Zhao, X.-J.; Zhang, Y.; Huang, W. A facile access to stiff epoxy vitrimers with excellent mechanical properties via siloxane equilibration. *J. Mater. Chem. A* **2018**, *6*, 10184–10188.
- (16) Liu, Q.; Jiang, L.; Zhao, Y.; Wang, Y.; Lei, J. Reprocessable and shape memory thermosetting epoxy resins based on silyl ether equilibration. *Macromol. Chem. Phys.* **2019**, *220*, 1900149.
- (17) Demongeot, A.; Mougner, S. J.; Okada, S.; Soulié-Ziakovic, C.; Tournilhac, F. Coordination and catalysis of Zn<sup>2+</sup> in epoxy-based vitrimers. *Polym. Chem.* **2016**, *7*, 4486–4493.
- (18) Chen, J.; Huang, H.; Fan, J.; Wang, Y.; Yu, J.; Zhu, J.; Hu, Z. Vitrimer chemistry assisted fabrication of aligned, healable, and recyclable graphene/epoxy composites. *Front. Chem.* **2019**, *7*, 632.

- (19) Shi, Q.; Yu, K.; Dunn, M. L.; Wang, T.; Qi, H. J. Solvent assisted pressure-free surface welding and reprocessing of malleable epoxy polymers. *Macromolecules* **2016**, *49*, 5527–5537.
- (20) Chen, G.-k.; Wu, K.; Zhang, Q.; Shi, Y.-c.; Lu, M.-g. Dual-responsive shape memory and thermally reconfigurable reduced graphene oxide-vitrimer composites. *Macromol. Res.* **2019**, *27*, 526–533.
- (21) Chen, M.; Zhou, L.; Wu, Y.; Zhao, X.; Zhang, Y. Rapid stress relaxation and moderate temperature of malleability enabled by the synergy of disulfide metathesis and carboxylate transesterification in epoxy vitrimers. *ACS Macro Lett.* **2019**, *8*, 255–260.
- (22) Han, J. R.; Liu, T.; Hao, C.; Zhang, S.; Guo, B. H.; Zhang, J. W. A catalyst-free epoxy vitrimer system based on multifunctional hyperbranched polymer. *Macromolecules* **2018**, *51*, 6789–6799.
- (23) Li, Y. Y.; Liu, T.; Zhang, S.; Shao, L.; Fei, M. G.; Yu, H.; Zhang, J. W. Catalyst-free vitrimer elastomers based on a dimer acid: robust mechanical performance, adaptability and hydrothermal recyclability. *Green Chem.* **2020**, *22*, 870–881.
- (24) Gosecki, M.; Gosecka, M. Boronic acid esters and anhydrides as dynamic cross-links in vitrimers. *Polymers* **2022**, *14*, 842.
- (25) Wu, S.; Yang, H.; Huang, S.; Chen, Q. relationship between reaction kinetics and chain dynamics of vitrimers based on dioxaborolane metathesis. *Macromolecules* **2020**, *53*, 1180–1190.
- (26) Röttger, M.; Domenech, T.; van der Weegen, R.; Breuillac, A.; Nicolaÿ, R.; Leibler, L. High-performance vitrimers from commodity thermoplastics through dioxaborolane metathesis. *Science* **2017**, *356*, 62–65.
- (27) Ricarte, R. G.; Tournilhac, F.; Leibler, L. Phase separation and self-assembly in vitrimers: hierarchical morphology of molten and semicrystalline polyethylene/dioxaborolane maleimide systems. *Macromolecules* **2019**, *52*, 432–443.
- (28) Ricarte, R. G.; Tournilhac, F.; Cloître, M.; Leibler, L. Linear viscoelasticity and flow of self-assembled vitrimers: the case of a polyethylene/dioxaborolane system. *Macromolecules* **2020**, *53*, 1852–1866.
- (29) Lucherelli, M. A.; Duval, A.; Avérous, L. Biobased vitrimers: towards sustainable and adaptable performing polymer materials. *Prog. Polym. Sci.* **2022**, *127*, 101515.
- (30) Yang, X.; Guo, L.; Xu, X.; Shang, S.; Liu, H. A fully bio-based epoxy vitrimer: self-healing, triple-shape memory and reprocessing triggered by dynamic covalent bond exchange. *Mater. Des.* **2020**, *186*, 108248.
- (31) Zych, A.; Tellers, J.; Bertolacci, L.; Ceseracciu, L.; Marini, L.; Mancini, G.; Athanassiou, A. Biobased, biodegradable, self-healing boronic ester vitrimers from epoxidized soybean oil acrylate. *ACS Appl. Polym. Mater.* **2021**, *3*, 1135–1144.
- (32) Xu, Y.-Z.; Fu, P.; Dai, S.-L.; Zhang, H.-B.; Bi, L.-W.; Jiang, J.-X.; Chen, Y.-X. Catalyst-free self-healing fully bio-based vitrimers derived from tung oil: strong mechanical properties, shape memory, and recyclability. *Ind. Crops Prod.* **2021**, *171*, 113978.
- (33) Zhong, L.; Hao, Y.; Zhang, J.; Wei, F.; Li, T.; Miao, M.; Zhang, D. Closed-loop recyclable fully bio-based epoxy vitrimers from ferulic acid-derived hyperbranched epoxy resin. *Macromolecules* **2022**, *55*, 595–607.
- (34) Liu, Y. L.; Wang, B. B.; Ma, S. Q.; Yu, T.; Xu, X. W.; Li, Q.; Wang, S.; Han, Y. Y.; Yu, Z.; Zhu, J. Catalyst-free malleable, degradable, bio-based epoxy thermosets and its application in recyclable carbon fiber composites. *Composites, Part B* **2021**, *211*, 108654.
- (35) Lorwanishpaisarn, N.; Srikhao, N.; Jetsrisuparb, K.; Knijnenburg, J. T. N.; Theerakulpisut, S.; Okhawilai, M.; Kasemsiri, P. Self-healing ability of epoxy vitrimer nanocomposites containing bio-based curing agents and carbon nanotubes for corrosion protection. *J. Polym. Environ.* **2022**, *30*, 472–482.
- (36) Brändle, A.; Khan, A. Thiol-epoxy 'click' polymerization: efficient construction of reactive and functional polymers. *Polym. Chem.* **2012**, *3*, 3224–3227.
- (37) De, S.; Khan, A. Efficient synthesis of multifunctional polymers via thiol-epoxy "click" chemistry. *Chem. Commun.* **2012**, *48*, 3130–3132.
- (38) Hayashi, M.; Katayama, A. Preparation of colorless, highly transparent, epoxy-based vitrimers by the thiol-epoxy click reaction and evaluation of their shape-memory properties. *ACS Appl. Polym. Mater.* **2020**, *2*, 2452–2457.
- (39) Smith, M. K.; Northrop, B. H. Vibrational properties of boroxine anhydride and boronate ester materials: model systems for the diagnostic characterization of covalent organic frameworks. *Chem. Mater.* **2014**, *26*, 3781–3795.
- (40) Li, C.; Chen, Y.; Zeng, Y.; Wu, Y.; Liu, W.; Qiu, R. Strong and recyclable soybean oil-based epoxy adhesives based on dynamic borate. *Eur. Polym. J.* **2022**, *162*, 110923.
- (41) Nikolic, G.; Zlatkovic, S.; Cakic, M.; Cakic, S.; Lacnjevac, C.; Rajic, Z. Fast Fourier transform ir characterization of epoxy gy systems crosslinked with aliphatic and cycloaliphatic eh polyamine adducts. *Sensors* **2010**, *10*, 684–696.
- (42) Ran, Y.; Zheng, L.-J.; Zeng, J.-B. Dynamic Crosslinking: An Efficient Approach to Fabricate Epoxy Vitrimer. *Materials* **2021**, *14*, 919.
- (43) Liu, Y.-Y.; He, J.; Li, Y.-D.; Zhao, X.-L.; Zeng, J.-B. Biobased, reprocessable and weldable epoxy vitrimers from epoxidized soybean oil. *Ind. Crops Prod.* **2020**, *153*, 112576.
- (44) Wang, D.-C.; Chang, G.-W.; Chen, Y. Preparation and thermal stability of boron-containing phenolic resin/clay nanocomposites. *Polym. Degrad. Stabil.* **2008**, *93*, 125–133.
- (45) Zeng, Y.; Liu, S.; Xu, X.; Chen, Y.; Zhang, F. Fabrication and curing properties of o-cresol formaldehyde epoxy resin with reversible cross-links by dynamic boronic ester bonds. *Polymer* **2020**, *211*, 123116.
- (46) Wang, M.; Yin, G.-Z.; Yang, Y.; Fu, W.; Díaz Palencia, J. L.; Zhao, J.; Wang, N.; Jiang, Y.; Wang, D.-Y. Bio-based flame retardants to polymers: a review. *Adv. Ind. Eng. Polym. Res.* **2023**, *6*, 132–155.
- (47) Shen, K. K. Review of recent advances on the use of boron-based flame retardants. In *Polymer Green Flame Retardants*; Elsevier, 2014; pp 367–388.
- (48) Kipcak, A. S.; Derun, E. M. A new approach on the evaluation of magnesium wastes in the magnesium borate synthesis using the novel method of ultrasonic irradiation. *Res. Chem. Intermed.* **2016**, *42*, 6663–6679.
- (49) Chakrabarty, K.; Chen, W.-C.; Baker, P. A.; Vijayan, V. M.; Chen, C.-C.; Catledge, S. A. Superhard boron-rich boron carbide with controlled degree of crystallinity. *Materials* **2020**, *13*, 3622.
- (50) Kipcak, A. S.; Senberber, F. T.; Moroydor Derun, E.; Piskin, S. Evaluation of the magnesium wastes with boron oxide in magnesium borate synthesis. *Int. J. Mater. Metall. Eng.* **2012**, *6*, 610–614.
- (51) Yang, P.; Sun, H.; Fan, H.; Shi, B. Novel environmentally sustainable cardanol-based plasticizers: synthesis and properties. *Polym. Int.* **2016**, *65*, 464–472.
- (52) Sheth, P.; Mestry, S.; Dave, D.; Mhaske, S. Isosorbide-derived boron- and phosphorus-containing precursors for flame-retardant epoxy coating. *J. Coating Technol. Res.* **2020**, *17*, 231–241.
- (53) Deng, P.; Shi, Y.; Liu, Y.; Liu, Y.; Wang, Q. Solidifying process and flame retardancy of epoxy resin cured with boron-containing phenolic resin. *Appl. Surf. Sci.* **2018**, *427*, 894–904.
- (54) Zhang, T.; Liu, W.; Wang, M.; Liu, P.; Pan, Y.; Liu, D. Synthesis of a boron/nitrogen-containing compound based on triazine and boronic acid and its flame retardant effect on epoxy resin. *High Perform. Polym.* **2017**, *29*, 513–523.
- (55) Chen, S.; Ai, L.; Zhang, T.; Liu, P.; Liu, W.; Pan, Y.; Liu, D. Synthesis and application of a triazine derivative containing boron as flame retardant in epoxy resins. *Arab. J. Chem.* **2020**, *13*, 2982–2994.